Astron. Astrophys. 325, 569–584 (1997)

ASTRONOMY
AND
ASTROPHYSICS

Dust evolution in protoplanetary accretion disks

Wolfgang Schmitt, Thomas Henning, and Rastislav Mucha

Max Planck Society, Research Unit "Dust in Star-forming Regions", Schillergäßchen 2-3, D-07745 Jena, Germany

Received 3 December 1996 / Accepted 28 March 1997

Abstract. The time evolution of dust particles in circumstellar disk-like structures around protostars and young stellar objects was investigated. For the first time, we coupled the dust evolution directly to the evolution of the disk and followed the influence of opacity changes due to collisional aggregation on the dynamics of the disk. For that purpose, we numerically simulated the dynamical evolution of a turbulent protoplanetary accretion disk described by a time-dependent one-dimensional (radial) "alpha" model. Within this model, the growth of dust grains due to coagulation was calculated by solving numerically the non-linear Smoluchowski equation. As physical processes leading to relative velocities between the grains, Brownian motion, turbulence, and drift motion were taken into account. In contrast to other studies, we especially considered particle-cluster agglomeration (PCA) as growth mode but also included cluster-cluster agglomeration (CCA) into our considerations. For time periods of 100 years and disk radii up to 100 AU, the mass distributions of coagulated dust grains were calculated. From these mass spectra, we determined the corresponding Rosseland mean dust opacities. The variations of the dust grain opacity drive changes in the energetic structure of the protoplanetary disk which again influences the accretion process itself. Our results show three evolutionary stages of the PCA process. For CCA particles, there is no dust growth after the disappearance of the smallest grains. The different characteristic timescales for the coagulation at different radii result in the restructuring of the dust region of the protoplanetary disks. Significant changes in the thermal and optical structure of the disk occur.

Key words: accretion disks – hydrodynamics – turbulence – methods: numerical – solar system: formation – planetary system

1. Introduction

In the present concept of the formation of our solar system, an accretion disk has been developed after the collapse of a gaseous nebula. In the 40's and 50's von Weizsäcker (1944, 1947, 1948) and Lüst (1952) and at the beginning of the 70's Shakura & Sunyaev (1973) and Lynden-Bell & Pringle (1974) formulated the mathematical basis for the standard model of a turbulent accretion disk surrounding a central object. The understanding of the evolution of the dust component in a protoplanetary nebula is crucial for explaining the formation of planetary systems. Safronov (1969) and Goldreich & Ward (1973) attributed the formation of planetesimals to a gravitational instability of a thin midplane dust subdisk. The protoplanetary disk was assumed to be quiescent and laminar at this evolutionary stage in order to allow for the sedimentation of dust particles towards the midplane. However, the protoplanetary nebula is expected to be turbulent at least at the beginning of its evolution. The very high Reynolds-number flow in a protoplanetary disk also suggests the existence of some kind of turbulence in there. It was suggested that a dust-opacity driven convective instability could be the mechanism supporting the turbulence in a protoplanetary disk (Lin & Papaloizou 1980; Weidenschilling 1984; Pollack et al. 1985; Lin & Papaloizou 1985). The estimation of the "strength" of the turbulence produced this way leads in terms of the "α" model to values of $\alpha \sim 0.01$ and lower (see, e.g., Cabot et al. 1987a, b). Morfill (1985) carried out one-dimensional calculations in radial direction for protoplanetary accretion disks including grain growth and sublimation of dust grains at higher temperatures. Mizuno et al. (1988) and Mizuno (1989) considered the growth process of dust grains in more detail: the evolution of the dust component is calculated including the radial drift, the transport and coagulation equation is solved numerically for a turbulent disk, and moreover the resulting opacities are determined. This calculation shows the decrease of the opacity due to grain growth, thus causing a shutdown of the convective instability. The authors suggest that due to infall of original grains on the disk, there can be a revival of the instability resulting in repeated changes between a quiescent and a turbulent state. However, in order to maintain angular momentum transport some long-living effective turbulence seems to be necessary. Those problems with the possibly short-living and weak convective instability suggest that other turbulence supporting mechanisms may be important, e.g., magnetic instability (e.g. Chandrasekhar 1961; Balbus & Hawley 1991; Stone et al. 1996), gravitative instabilities (e.g. Larson 1984; Lin & Pringle 1987), or a infall-driven local shear instability (e.g. Cassen & Moosman 1981). Even weak turbulence is sufficient to prevent the dust layer from becoming gravitationally unstable (Weiden-

schilling 1988). Furthermore, particles which are small enough to be coupled to the turbulent motion are prevented from sedimentation. Cuzzi et al. (1993) showed that the Goldreich-Ward instability is unlikely to occur until objects have already accreted by some other process to the mass of the largest known meteorite samples, if at all. This supports the coagulation scenario, combined with grain and vapour transport processes. All the time, however, the grains were assumed to be spheres – an assumption which is not longer correct if the coagulation process gets ahead. Various authors pointed out that the internal structure of the dust grains influences the opacities significantly (see, e.g., Preibisch et al. 1993; Ossenkopf & Henning 1994; Henning & Stognienko 1996). Calculations on the coagulation of dust particles having a fluffy structure were performed by Ossenkopf (1993) for the cores of cold molecular clouds (see also Weidenschilling & Ruzmaikina 1994). These investigations resulted in constraints on the dust size spectrum and its influence on the opacity (Ossenkopf & Henning 1994).

In this paper, we investigate the dust evolution in protoplanetary accretion disks. For the first time, we couple the dust evolution directly to the evolution of the disk and follow the influence of opacity changes due to collisional aggregation on the dynamical behaviour of the disk.

In Sect. 2-4, our basic assumptions, model equations and numerical methods are described. In particular, in Sect. 2, we first point out our idea of coupling of disk evolution with the dust evolution. In Sect. 3, we especially treat the protoplanetary accretion disk. Then, in Sect. 4, we deal with dust evolution, and gas and dust opacities. In Sect. 5, the results of our numerical simulations are presented and discussed. Finally, in Sect. 6, we draw our conclusions. Additionally, a description of processes involved in the evolution of dust grains is given in an Appendix.

2. Coupling of disk and dust evolution

In order to understand the decisive physical processes leading to the evolution of protoplanetary systems, on the one hand we have modelled in computer simulations a turbulent accretion disk around a protostellar object using a one-dimensional (radial) time-dependent model. On the other hand, we are dealing with dust coagulation – the growth process of cosmic dust grains. Since in protoplanetary disks, dust grains – as long as they exist – dominate the opacity and the opacity again influences the disk evolution, we have created a model coupling disk and dust evolution (subsequently referred to as DISCO = accretion DISk + dust COagulation). The basic idea behind that is having the disk structure to calculate first the mass distribution of dust grains due to collisional aggregation and then to determine the corresponding dust opacities from these dust spectra for an evolving protoplanetary disk. Finally, these opacities are used to calculate the energetic structure of the disk which guarantees the feedback of the dust distribution on the hydrodynamic evolution of the disk.

In the following, we will first describe our protoplanetary accretion disk model and then represent the dust coagulation model in more detail.

3. Protoplanetary accretion disk

For the description of the structure of a geometrically thin protoplanetary accretion disk, we use the hydrodynamical equations of a viscous fluid. Since detailed derivations and explanations of these equations can be found in the literature (e.g. Ruden & Pollack 1991; Frank et al. 1992) we will be brief on this point.

3.1. Disk structure equations

The evolution of the disk due to viscous processes is described by the nonlinear diffusion equation for the surface density Σ

$$\frac{\partial \Sigma}{\partial t} = \frac{3}{r}\frac{\partial}{\partial r}\left[r^{\frac{1}{2}}\frac{\partial}{\partial r}\left(\nu\Sigma r^{\frac{1}{2}}\right)\right]. \tag{1}$$

For the kinematic viscosity ν we adopt the "alpha"-prescription (Shakura & Sunyaev 1973)

$$\nu = \frac{2}{3}\alpha c_s H, \tag{2}$$

where we assume the parameter α to be 0.01 which is a value consistent with the observed lifetimes of disks. The structure of the disk in vertical direction is described by the following five equations: The gas density ρ is defined by

$$\rho = \frac{1}{2}\frac{\Sigma}{H}. \tag{3}$$

The disk half-thickness H is determined by the hydrostatic equilibrium in the disk

$$H = \frac{c_s}{\omega_K}, \tag{4}$$

where the Keplerian angular velocity ω_K is given by $\left(GM_\star/r^3\right)^{\frac{1}{2}}$. For the mass of the central object $M_\star$ we assume one solar mass. The isothermal sound speed c_s is defined by

$$c_s^2 = \frac{k_B}{\mu m_p}T. \tag{5}$$

The quantities k_B, m_p, and μ denote the Stefan-Boltzmann constant, the proton mass, and the mean molecular weight, respectively. Assuming an optically thick disk, the gas temperature in the midplane T is related to the effective temperature T_e by

$$T^4 = \frac{3}{4}\tau T_e^4, \tag{6}$$

where τ is the optical depth. The local energy balance between energy generated by viscous dissipation and radiative losses from both disk's surfaces is described by

$$2\sigma T_e^4 = \frac{9}{4}\nu\Sigma\omega_K^2, \tag{7}$$

where σ is the Stefan-Boltzmann constant. The optical depth from the midplane to the disk's surface τ is given by

$$\tau = \frac{1}{2}\Sigma\kappa_R, \tag{8}$$

where $\kappa_R = \kappa_R(\rho, T)$ denotes the Rosseland mean opacity. The goal of this paper is to take into account the opacity changes of growing dust grains due to coagulation. Thus, in our DISCO model, the opacity is the connecting link between a "pure" disk model and a "pure" dust coagulation model.

3.2. Numerical method and boundary conditions

To solve the system of the eight coupled Eqs. (1-8), we proceed on the method proposed by Bath & Pringle (1981). Applying the following transformation for the diffusion equation (1) $X = 2r^{\frac{1}{2}}$ and $S = \Sigma X$ one yields

$$\frac{\partial S}{\partial t} = \frac{12}{X^2}\frac{\partial^2}{\partial X^2}(S\nu). \tag{9}$$

We solve this equation with a fully implicit scheme needing boundary conditions at the inner and outer radii of the disk. At the inner radius we assume no viscous stress to allow matter to fall freely onto the protostar by setting $\Sigma = 0$. For the outer radius we choose a spatial grid large enough that the matter can freely diffuse outwards.

For all simulations we fixed the radius of the protoplanetary disk to $R_{\rm disk} = 1.5 \cdot 10^{15}$ cm and assumed the radius of the central object to be eight times the solar radius which is the radius of a one solar mass deuterium protostar (Shu et al. 1987).

Although the initial conditions for the disk evolution are poorly constrained, our numerical simulations start from a distribution of the surface density which is the steady-state solution of the disk model (e.g. Frank et al. 1992) with the prescribed opacity given by the initial dust distribution. These solutions are made up to a radius of $6 \cdot 10^{14}$ cm. Between this radius and the outer radius of the disk, we extrapolated the physical quantities to match the interstellar conditions at the outer boundary.

Once the surface density, $\Sigma(r, t)$, is calculated all the remaining disk quantities can be deduced algebraically.

As an additional numerical complication – in our special case of coupling the disk evolution and the dust evolution – we have not only to solve the disk structure equations but we also have to solve the integrodifferential equation of the dust coagulation and to calculate the dust opacities for certain timesteps simultaneously.

4. Dust evolution

Concerning the evolution of dust grains embedded in a gaseous environment, the approach we adopted is to describe the whole grain ensemble by a dust distribution function. For the sake of simplicity in the subsequent formulas, we restrict ourselves to a 3-parameter distribution function $f(\boldsymbol{r}, t, V)$, where $\boldsymbol{r}, t, V$ are the space vector, the time and a parameter characterizing the size of the dust particle (compact volume), respectively. However, the interactions between particles and particles and gas are stochastic, e.g., relative velocities of the dust particles are induced by chaotic motions of the gas (thermal and turbulent). This means that our distribution function f is a stochastic variable and we should use the Chapman-Kolmogorov equation (Gardiner 1990) for the probability density p of the dust distribution

$$\frac{\partial}{\partial t}\,p(f,t) = -\frac{\partial}{\partial f}\left\{a(f,t)\,p(f,t)\right\} + \frac{\partial^2}{\partial f^2}\left\{b(f,t)\,p(f,t)\right\} + \int df'\left\{w(f,f',t)\,p(f',t) - w(f',f,t)\,p(f,t)\right\}. \tag{10}$$

Here, we assumed that the stochastic processes are of Markovian type, i.e., they depend only on the newest history of the system and not on the whole one. This equation nicely illustrates that there are 3 types of evolutionary processes. The first term on the r.h.s. represents advection, i.e., the deterministic part of the evolution, the second one describes the stochastic diffusion, and finally the last one represents jump processes. The quantities a, b, and w are the corresponding transition probabilities. The differential Chapman-Kolmogorov equation is very difficult to solve analytically or even numerically. Approximating it by a stochastic equation (Gardiner 1990) gives an equation of the following form

$$df(\boldsymbol{r}, t, V) = A(\boldsymbol{r}, t, V)\,dt + B(\boldsymbol{r}, t, V)\,dW \tag{11}$$

but the problems of solving such an equation would remain. The variable dW is the stochastic differential of a Wiener process (Gardiner 1990), also called noise and the coefficients A and B are related to a, b, w. We do not show this dependence explicitly because it does not matter for the subsequent analysis. An obvious procedure is to ignore the second-stochastic term on the r.h.s. of Eq. (11) which results in an fully deterministic equation. More exactly, the sketched procedure corresponds to averaging the stochastic equation over a large number of realizations of the dust ensemble. Then, we obtain the statistical equation which is also called kinetic equation

$$\frac{df}{dt}\,f(\boldsymbol{r}, t, V) = A(\boldsymbol{r}, t, V). \tag{12}$$

For a more detailed discussion we refer to Mucha (in prep.). The fact that our basic equation is a statistic equation should be always borne in mind (see Sect. 5).

In order to determine the total time derivative of f and the source term A in the basic Eq. (12) we have to specify the processes taking part in the evolution of the dust particles and the environment they are embedded in. As the environment, we choose the 1D protoplanetary accretion disk (see Sect. 2).

4.1. General formulation

The evolution of the dust population can be described by the equation

$$\frac{\partial}{\partial t}\,f(\boldsymbol{r}, t, V) + \frac{\partial}{\partial \boldsymbol{r}}\left(\boldsymbol{v}_d f(\boldsymbol{r}, t, V)\right) + \frac{\partial}{\partial V}\left(\dot{V} f(\boldsymbol{r}, t, V)\right) = S_{\rm cgn} + S_{\rm cdn} + S_{\rm acc} + S_{\rm scn} + S_{\rm chd} + S_{\rm acr} \equiv S, \tag{13}$$

where

$$\dot{V} = W_{\rm acc} + W_{\rm scn} + W_{\rm chd} \equiv W_{\rm ascd} \tag{14}$$

describes the continuous change of the volume (mass) of the dust grains due to the accretion of molecules onto preexisting grains, sublimation/condensation, and chemical destruction. The term S includes jump-like changes in the mass distribution. It is composed of coagulation, collisional destruction, accretion of molecules, sublimation/condensation, chemical destruction, and accretion from the remaining cloud surrounding the disk. The detailed expressions are given in the Appendix.

In principle, we have to model two kinds of processes: continuous and jump-like changes of the compact volume. To determine which of the mass (volume) changing processes belongs to a particular category is a matter of convenience and mass (volume) scales involved. We define a process to be continuous if the change of the compact volume during one interaction is at least by an order of magnitude less than the volume of the smallest dust grain considered. From that, one sees why there are no continuous counterparts to coagulation and collisional destruction of dust. In this model, we do not explicitly compute the collisional destruction of dust particles and changes of V due to accretion, sublimation/condensation and chemical destruction (see Appendix). This will be done in forthcoming investigations.

4.2. Dust motion

The motion of dust grains in a gaseous environment is influenced by the drag force due to collisions with the gas molecules (Epstein 1923; Baines et al. 1965). This force $\boldsymbol{F}$ can be expressed by

$$\boldsymbol{F} = -\frac{\boldsymbol{v}_d - \boldsymbol{v}_g}{\tau_f}, \tag{15}$$

where τ_f is the characteristic timescale of the change of momentum of a dust grain, the so-called characteristic friction timescale. The quantities $\boldsymbol{v}_d$ and $\boldsymbol{v}_g$ are the dust and gas velocity, respectively. The friction time depends on particle size, density, physical parameters of the gaseous environment and the relative dust-gas velocity. For spheroidal compact gas grains, there are two main regimes which are called the Epstein and the Stokes regime. The first one is valid for small and the second one for large particles. The corresponding friction times depend on the "size" of the particle V/A relative to the mean free path λ of the gas molecules (see, e.g., Weidenschilling 1977; Ossenkopf 1993). Here, V is the compact volume and A the projected area of the particle. For the Epstein regime $\frac{V}{A} < 3\,\lambda$, the friction time is given by

$$\tau_f = \frac{\sqrt{\pi}}{2}\,\frac{V}{A}\,\frac{\rho_s}{\rho_g} \tag{16}$$

and for the Stokes regime $\frac{V}{A} > 3\,\lambda$ by

$$\tau_f = \frac{8}{3}\,\frac{\sqrt{\pi}}{2}\,\frac{V}{A}\,\frac{\rho_s}{\rho_g}\left(C_D\,|\boldsymbol{v}_d - \boldsymbol{v}_g|\right)^{-1}, \tag{17}$$

where ρ_d, ρ_g and C_D denote the density of a dust particle, the gas density and the drag coefficient (Baines et al. 1965). The mean free path λ in the protoplanetary nebula is of the order of about 10^5 cm. This means that we only have to consider the Epstein regime for our particle sizes. The grains are considered to have an internal structure. They are porous and we model them as fractals (see Sect. 4.3). Thus, it arises the question of the validity of the Epstein formula for such grains. The main problem is to figure out whether the overall functional dependence for fractal grains is the same as for spheroidal ones or not. In view of the present lack of information on this subject, we also will use the Epstein law for these particles. This is probably not a bad approximation for particles composed of many subparticles as recently shown by Blum et al. (1996). However, we expect that there may be another constant in Eq. (16). We also suppose that for very irregular grains composed only of a couple of subgrains, there can be a significant change in functional behaviour compared with Eq. (16). In spite of these problems, we understand the Epstein formula as a kind of first approximation for the momentum exchange between gas and grains.

Having specified the friction force, we can now formulate the equation of motion of dust in our protoplanetary accretion disk. Since mainly relative velocities between dust and gas and between dust grains are of importance for our investigations, we just give the formulas for the components of the relative grain-gas velocity in cylindrical coordinates (see, e.g., Morfill 1985).

$$v_{dr} - v_{gr} = \frac{\tau_f}{\rho_g}\,\frac{\partial P}{\partial r} + \frac{\tau_f\,v_{g\phi}^2}{r}\left(\frac{1}{1+\frac{\tau_f\,v_{dr}}{r}} - 1\right) \tag{18}$$

$$v_{d\phi} - v_{g\phi} = v_{g\phi}\left(\frac{\tau_f\,v_{dr}}{r}\right)^{-1} \tag{19}$$

$$\frac{d(v_{dz} - v_{gz})}{dt} = \frac{dv_{dz}}{dt} = -z\,\Omega_K^2 - \frac{v_{dz}}{\tau_f}. \tag{20}$$

In Eqs. (18-20) we assumed that no back reaction of the dust onto the gas motion takes place. In Eq. (20) $v_{gz} = 0$ is the direct consequence of the vertical hydrostatic equilibrium in our disk model. Furthermore, we assumed that the timescales on which we follow a dust grain are large compared to the friction time and small compared to the viscous time scale. For two limiting cases, $\frac{\tau_f\,v_{dr}}{r} = \tau_f\,\Omega_K \ll 1$, and $\frac{\tau_f\,v_{dr}}{r} = \tau_f\,\Omega_K \gg 1$, one can obtain an analytical solution for the Eqs. (18-20). These limits correspond to small and large particles (see, e.g., Weidenschilling 1977; Morfill 1985). In our calculations, we consider the evolution of particles until they have grown to a size of $V \sim 1\ cm^3$ ($\tau_f\Omega_K \lesssim 10^{-2}$). Consequently, we are in the regime of small particles. For Eqs. (18-20) we then obtain

$$v_{dz} = -z_1\,\Omega_K^2\,\tau_f + z_2\,(\Omega_K^2\,\tau_f^2 - 1)\,\tau_f^{-1} \tag{21}$$

$$z_1 = C_1\ \exp(-\Omega_K^2\,\tau_f\,t) \tag{22}$$

$$z_2 = C_2\ \exp((\Omega_K^2\,\tau_f^2 - 1)\,\tau_f^{-1}\,t), \tag{23}$$

which reduces for $t \gg \tau_f$ to

$$v_{dz} = -z\,\Omega_K^2\,\tau_f. \tag{24}$$

Eqs. (18-19) reduce to

$$v_{dr} = \left(v_{gr} + \frac{\tau_f}{\rho_g} \frac{\partial P}{\partial r} \right) \left(1 + \Omega_K^2 \, \tau_f^2 \right)^{-1} \tag{25}$$

$$v_{d\phi} = v_{g\phi} \left(1 + \frac{\tau_f \, v_{dr}}{r} \right)^{-1} . \tag{26}$$

These drift velocities are used in Sect. 5.2.1 for determining the characteristic advection time. Moreover, the relative drift velocities of the dust particles co-determine their collisional probability (see also Sect. 4.4).

We now direct our attention from the deterministic motion of the dust material to one aspect its stochastic motion. Namely, due to the induced random dust grain velocities by the turbulent motion of the protoplanetary disk gas, the grains are transported diffusively. At the beginning of Sect. 4, we introduced a statistical evolution equation for the dust mass (compact volume) distribution function f by ignoring (averaging out) the stochastic term. We assume that the stochastic component of the kinetic evolution equation is induced by the (magneto-)hydrodynamical turbulence in the protoplanetary nebula. Furthermore, we consider that the change of the compact volume V is not explicitly stochastic, i.e., the evolutionary path in mass (compact volume) space is deterministic. This corresponds to setting the stochastic part of the source term in Eq. (13) to zero. For the sake of simplicity, we do not explicitly express the V dependence in the next equations.

We use the Reynolds method of describing the turbulent flow. Here, we write $\boldsymbol{v}_d$ as the sum of its mean $\bar{\boldsymbol{v}}_d$ and its fluctuating part $\boldsymbol{v}'_d$,

$$\boldsymbol{v}_d = \bar{\boldsymbol{v}}_d + \boldsymbol{v}'_d, \tag{27}$$

and the same for f

$$f = \bar{f} + f'. \tag{28}$$

Introducing this ansatz into Eq. (13) and taking its average we obtain (in Cartesian coordinates)

$$\frac{\partial \bar{f}(\boldsymbol{r},t)}{\partial t} + \frac{\partial}{\partial x_i} \left(\bar{v}_{di}(\boldsymbol{r},t) \, \bar{f}(\boldsymbol{r},t) \right) + \frac{\partial}{\partial x_i} \left(\overline{v'_{di}(\boldsymbol{r},t) \, f'(\boldsymbol{r},t)} \right) + \frac{\partial}{\partial V} \left(\dot{V} \, \bar{f}(\boldsymbol{r},t) \right) = S, \tag{29}$$

which is the equation describing the evolution of the mean distribution function, i.e., the mean field equation accounting for the effect of advection and diffusion. After subtracting Eq. (29) from Eq. (13), we get an equation governing the stochastic fluctuations f'

$$\frac{\partial f'(\boldsymbol{r},t)}{\partial t} + \frac{\partial}{\partial x_i} \left(v'_{di}(\boldsymbol{r},t) \, \bar{f}(\boldsymbol{r},t) + \bar{v}_{di}(\boldsymbol{r},t) \, f'(\boldsymbol{r},t) \right) + \frac{\partial}{\partial x_i} \left(v'_{di}(\boldsymbol{r},t) \, f'(\boldsymbol{r},t) - \overline{v'_{di}(\boldsymbol{r},t) \, f'(\boldsymbol{r},t)} \right) + \frac{\partial}{\partial V} \left(\dot{V} \, f'(\boldsymbol{r},t) \right) = 0. \tag{30}$$

We restrict ourselves to the second order correlations approximation (Krause & Rüdiger 1974) in order to close our system of equations. Therefore, we approximate the second order term in Eq. (30) in the following way

$$\frac{\partial}{\partial x_i} \left(v'_{di}(\boldsymbol{r},t) \, f'(\boldsymbol{r},t) \right) - \frac{\partial}{\partial x_i} \left(\overline{v'_{di}(\boldsymbol{r},t) \, f'(\boldsymbol{r},t)} \right) = -d \, \frac{\partial f'}{\partial x_i}. \tag{31}$$

Here, we assumed that the small-scale stochastic fluctuations provide a background for the modes we focus. These small scales are supposed to be sufficiently homogeneous and isotropic, i.e., they influence larger-scale fields only through some scalar diffusivity d, e.g., the Brownian one. Thus, the equation to be solved is

$$\frac{\partial f'(\boldsymbol{r},t)}{\partial t} + \frac{\partial}{\partial x_i} \left(\bar{v}_{di}(\boldsymbol{r},t) \, f'(\boldsymbol{r},t) \right) - d \, \Delta f' + \frac{\partial}{\partial V} \left(\dot{V} \, f'(\boldsymbol{r},t) \right) = -\frac{\partial}{\partial x_i} \left(v'_{di}(\boldsymbol{r},t) \, \bar{f}(\boldsymbol{r},t) \right). \tag{32}$$

This quasi-linear equation can now be treated with the Green's function method of the mean-field electrodynamics (Krause & Rädler 1980). The method yields a general solution of the following form

$$f'(\boldsymbol{r},t) = -\int\int d\boldsymbol{\delta} d\tau \, G(\boldsymbol{r}, \boldsymbol{r}+\boldsymbol{\delta}, t, t+\tau) \times \frac{\partial}{\partial (r_j + \delta_j)} \left(v'_{dj}(\boldsymbol{r}+\boldsymbol{\delta}, t+\tau) \, \bar{f}(\boldsymbol{r}+\boldsymbol{\delta}, t+\tau) \right), \tag{33}$$

where G is the Green's function of Eq. (32). Having obtained at least a formal solution to the fluctuating part of the distribution function, we recall Eq. (29) describing the evolution of the mean of distribution function $\bar{f}$ where we replace $\bar{f}$ with f in the following. In analogy to the kinetic theory of gases, we expect gradient-like diffusive transport of the dust particles in the nebula. However, there is no obvious reason why only first derivatives should occur, so we implicitly define the coefficients of diffusive transport to be

$$\overline{v'_{di}(\boldsymbol{r},t) \, f'(\boldsymbol{r},t)} = -D_{ij} \, \frac{\partial f(\boldsymbol{r},t)}{\partial x_j} - D_{ijk} \, \frac{\partial f(\boldsymbol{r},t)}{\partial x_j \partial x_k} + \ldots \tag{34}$$

This expression reduces to the simple diffusion ansatz if no derivatives higher than first order exist. To determine the eddy dust diffusion tensors, we have to calculate the correlation between velocity and gradient of the dust distribution function standing on the left side of the last equation. The averages of products between vector quantities lead to tensors and between vector and scalar quantities to correlation vectors. Thus, in our case, we have the two-point-two-time correlation tensor of the dust velocity field

$$Q^d_{ij}(\boldsymbol{r}, \boldsymbol{r}+\boldsymbol{\delta}, t, t+\tau) = \overline{v'_{di}(\boldsymbol{r},t) v'_{dj}(\boldsymbol{r}+\boldsymbol{\delta}, t+\tau)}, \tag{35}$$

and the two-point-two-time correlation vector

$$q^d_i(\boldsymbol{r}, \boldsymbol{r}+\boldsymbol{\delta}, t, t+\tau) = \overline{v'_{di}(\boldsymbol{r},t) f'(\boldsymbol{r}+\boldsymbol{\delta}, t+\tau)}. \tag{36}$$

Inserting Eq. (33) into Eq. (34) yields

$$\overline{v'_{di}(\boldsymbol{r},t)\,f'(\boldsymbol{r},t)} = -\int\int d\boldsymbol{\delta}d\tau\left\{G(\boldsymbol{r},\boldsymbol{r}+\boldsymbol{\delta},t,t+\tau)\right.$$
$$\left.\times\frac{\partial}{\partial(r_j+\delta_j)}\left(Q^d_{ij}(\boldsymbol{r},\boldsymbol{r}+\boldsymbol{\delta},t,t+\tau)\bar{f}(\boldsymbol{r}+\boldsymbol{\delta},t+\tau)\right)\right\}. \quad (37)$$

In some special cases, it is possible to evaluate the convolution integral on the r.h.s. of this equation analytically and, thus, to obtain a closed expression for the dust particles diffusion tensors D_{ij}, D_{ijk} and so on. For the numerical treatment of Eq. (37) see Mucha (in prep.).

For illustration purposes, we now approximate the diffusion tensor for a special case. We set $W_{\rm ascd} = 0$ (see Eq. 14) and assume two scales of the turbulence. This means that the fluctuations must be on much smaller scales than the mean field, i.e., we have for the correlation length $l_c < l$ and for the correlation time $\tau_c < t$. It is assumed that the mean quantities can be expressed by a Taylor expansion up to the first order in any space region of the size of l_c and constant in any time interval of duration of τ_c. Furthermore, we assume that the stochastic quantities are sums of a part not influenced by the mean motion v^0_d, f^0 (in the following called 0-th order contribution) and of a part describing the 1-st order influence of the mean motion v^1_d, f^1 (in the following called 1-st order contribution) on the turbulence. For the sake of simplicity, here, we only develop an expression for the 0-th order contribution, i.e., without any influence of the mean motion on the turbulence. For the 1-st order contribution we refer to Mucha (in prep.). Now, we have to specify the gas turbulence model. The gas turbulence is believed to be very important for the angular momentum. In the corresponding angular momentum conservation law, only the components of the two-point-two-time correlation tensor of the gas velocity field Q^g_{ij} exist which contain the cross correlations, i.e., $i \neq j$. There is no reason why the turbulence should be isotropic. At least, two preferred directions are given by gravity and rotation axes. Ignoring this possibility in this paper, we take the simplest possible representation of the gas turbulence, i.e., the homogeneous steady isotropic incompressible and mirror-symmetric one. In this case, all mean quantities representing the gas flow are isotropic tensors.

Furthermore, we have to figure out the correspondence between gas-induced dust turbulence and the gas turbulence itself (see, e.g., Völk et al. 1980). Our approximation yields after some manipulations

$$Q^{0d}_{ij}(\boldsymbol{r},0,t,0) = \int\int \frac{\hat{Q}^{0g}_{ij}}{1+\omega^2\tau_f^2}\,d\boldsymbol{k}d\omega, \quad (38)$$

where $\hat{Q}^{0g}_{ij}(\boldsymbol{k},\omega)$ is the Fourier transform of the two-point-two-time correlation tensor of the original turbulent gas velocity field.

With the assumption that the character of the stochastic dust motions is the same as for the gas, we assume particularly isotropy and, furthermore, no cross correlations. Then the diffusion can be described by a single scalar turbulent diffusivity D. From the correlation between velocity and the distribution function Eq. (36), we see that the eddy diffusivity is given by

$$D^{(0)} = \frac{1}{3}\int\int \frac{\hat{Q}^{0d}_{ii}}{-i\,\omega + k^2\,d}\,d\boldsymbol{k}d\omega. \quad (39)$$

Introducing a Kolmogorov-like turbulence with power spectra satisfying (e.g. Lin 1961; Landau & Lifschitz 1988; Krause & Rüdiger 1974)

$$\hat{Q}^{(0)g}_{ii} = \frac{P(k)}{4\,\pi\,k^2}\,\frac{1}{\tau_c\left(\omega^2+\tau_c^{-2}\right)}, \quad (40)$$

we finally obtain

$$D^{(0)} = \frac{1}{3}\int \frac{\tau_c\,P(k)}{(k^4\tau_f^2d^2-1)(k^4\tau_c^2d^2-1)}\,dk$$
$$+\frac{d}{3}\int \frac{\tau_c\,k^2\,P(k)}{\tau_f^2-\tau_c^2}$$
$$\times\left(\frac{\tau_f^3}{k^4\tau_f^2d^2-1}-\frac{\tau_c^3}{k^4\tau_c^2d^2-1}\right)dk. \quad (41)$$

For more details concerning the above calculations we refer to Mucha (in prep.). For different approaches on calculating the diffusion constant, we refer to, e.g., Cuzzi et al. (1993) and Dubrulle et al. (1995). The diffusion constant we just obtained can be used for determining the characteristic diffusion time. We recall that the Brownian diffusivity is already included in the formula (41), through the parameter d.

Finally, we determine the relative velocities which along with the cross sections of the dust particles determine their collisional probability. Applying the results of Ossenkopf (1993) for the relative velocities in the cold molecular cloud cores onto protoplanetary accretion disks shows that only thermal (Brownian) $v_{\rm Brown}$, turbulent v_{turb}, and drift-induced relative velocities are of importance. The presence of only two drift velocities, the radial and azimuthal ones, comes from the restriction of the hydrodynamical 1D disk model, averaged over the vertical z direction. We assume that there are no charges on the grains. Also if a small fraction of the grains is charged, the slowing down of the coagulation due to predominately negative charges on the charged grains would be very small (Ossenkopf 1993). Thus, the relative velocity is given by

$$v_{\rm rel} = \left\{\left[\langle v_{\rm Brown}(\rho_b\,V_1)\rangle + \langle v_{\rm Brown}(\rho_b\,V_2)\rangle\right] + \langle\Delta v_{12}^2\rangle\right.$$
$$+\left[(v_{dr}(\rho_b\,V_1)-v_{dr}(\rho_b\,V_2))^2\right.$$
$$\left.\left.+(v_{d\phi}(\rho_b\,V_1)-v_{d\phi}(\rho_b\,V_2))^2\right]\right\}^{\frac{1}{2}}, \quad (42)$$

where the radial v_{dr} and the azimuthal $v_{d\phi}$ velocities are determined by the Eqs. (25-26) and the relative Brownian velocity is

$$\langle v_{\rm Brown}\rangle = \left(\frac{8k_BT(V_1+V_2)}{\pi\rho_b\,V_1\,V_2}\right)^{\frac{1}{2}}. \quad (43)$$

For the calculation of the random relative velocity between two dust grains induced by the turbulent motion of the gas, we adopt the approach of Völk et al. (1980) (see also Morfill 1985) which leads to an approximative analytical formula

$$\langle \Delta v_{12}^2 \rangle = \langle \delta v_g^2 \rangle (\varepsilon_1 + \varepsilon_2 - 2\varepsilon_1 \varepsilon_2). \quad (44)$$

Assuming a homogeneous, isotropic, incompressible fully developed turbulence (Kolmogorov-spectrum $P_G \sim k^{-\frac{5}{3}}$), we have

$$\langle \delta v_g^2 \rangle = 2 \int_{k_0}^{k_s} P_G(k) dk. \quad (45)$$

Here, k_s is the scaled wavenumber $k_s = Re^{\frac{3}{4}} k_0$ giving a cutoff for the turbulence on the scale of the molecular motion, where the dissipation of the energy transfered through the turbulent cascade occurs (Markiewicz et al. 1991). The wavenumber of the largest structure present in the turbulence spectra, also called the largest eddy, is approximated by the pressure scale height in the 1D α-model of the disk, i.e., $k_0 = \frac{2\pi}{H}$. Furthermore, the factors ε_i are functions of ratios of the characteristic friction time τ_{f_i} of a gas particle and of the typical correlation time of the turbulence $\tau_{k_0} = (\alpha c_s k_0)^{-1}$ which are given by

$$\varepsilon_i \equiv \left(1 + \frac{\tau_{f_i}}{\tau_{k_0}} \right)^{-1}. \quad (46)$$

In general, for the smaller particles in the distribution (a $\sim$ 5 nm-100 μm), the Brownian relative velocities dominate because they all are fully coupled to the turbulence. For larger grains, the turbulence induced relative velocities are most important. Only for the largest particles produced ($V \gtrsim 1\mathrm{cm}^{-3}$) the drifts become more important.

4.3. Dust model

The dust grains are supposed to grow mainly due to cohesive sticking during the collisions. This process leads to the formation of aggregates of particles. As long as they do not undergo some restructuring causing compaction of conglomerates of the particles, the structure of the clusters is likely to be fluffy. Given the presently incomplete understanding of the compaction process, we ignore it in this work. The mean free path of the dust particles in an accretion disk is much higher then the sizes of aggregates, i.e., the grains approach each other on ballistic trajectories. There are two limiting cases for growth models namely particle-cluster aggregation (PCA) and cluster-cluster aggregation (CCA). For the most of our calculations, we assume that the particles are PCA's (see Sect. 5.1). In order to model the structure-characterizing parameters, like projected area (A/V) and collisional cross sections σ, we use the fractal model of Ossenkopf (1993).

Dust is assumed to be composed of a carbon-silicate mixture with a relative abundance $\eta_C = 0.47$ of carbon in the total refractory component. To simplify matters, we suppose for the dust only one identical sublimation temperature of $T_{\mathrm{crit}} = 1500$ K. The opacities of the coagulated grains were calculated by an effective medium theory combined with a core-mantle approach (Ossenkopf 1991). The corresponding bulk densities are $\rho_{b_C} = 2.3\, g\, cm^{-3}$ and $\rho_{b_{\mathrm{Si}}} = 3.2\, g\, cm^{-3}$ for amorphous carbon and the silicates, respectively. The inverse monochromatic extinction coefficients C_{ext} were averaged over the wavelength to obtain the Rosseland mean opacities:

$$\frac{1}{\kappa_R} = \int_0^\infty \left(\frac{1}{C_{\mathrm{ext}}(\lambda)/\rho} \right) \frac{\partial B_\lambda(T)}{\partial T} d\lambda \Big/ \int_0^\infty \frac{\partial B_\lambda(T)}{\partial T} d\lambda \quad (47)$$

where B_λ is the Planck function. The Rosseland mean opacities of the gas in the dust-free parts of the nebula were taken from Bell & Lin (1994). For a more detailed model of the dust opacities we refer to Henning & Stognienko (1996).

The bonds between constituting particles holding large aggregates together are relatively week to withstand the temperatures during the formation of the protoplanetary disk from the collapsing cloud. Particularly, the ice mantles should have been evaporated during this evolutionary stage. As the consequence, the size distribution of dust grains which evolved in the cold dense molecular cloud cores (Rossi et al. 1991; Ossenkopf 1993) is assumed to be destroyed. Therefore, the interstellar MRN distribution (Mathis et al. 1977)

$$f(\boldsymbol{r}, t_0, V) = C(\boldsymbol{r})\, V^{-\frac{11}{6}}\, dV, \quad (48)$$

is a reasonable initial condition for our calculations. However, we should stress that the investigations of the initial conditions for the growth process needs more detailed investigations (see also Sect. 5). The local constant $C(\boldsymbol{r})$ is determined by the requirement that

$$\rho_d(\boldsymbol{r}, t_0) = C(\boldsymbol{r}) \int_{V_{\mathrm{min}}^0}^{V_{\mathrm{max}}^0} V^{-\frac{11}{6}}\, \rho_b\, dV, \quad (49)$$

where

$$\rho_b = \eta_C\, \rho_{b_C} + (1 - \eta_C)\, \rho_{b_{\mathrm{Si}}}, \quad (50)$$

and V_{min}^0 and V_{max}^0 are 5.24×10^{-19} cm^3 (a $\approx$ 5 nm) and 5.24×10^{-10} cm^3 (a $\approx 5\mu$m), respectively.

For the regions which were all too hot for the dust ($T_{\mathrm{crit}} \geq 1500$ K) at the beginning of the disk evolution, we assume for the sake of simplicity that the initial dust distribution in the form of Eq. (48) establishes instantaneously after the temperature drops below the critical value T_{crit} (see also Sect. A.2.3). We are aware of the fact that this is a rather crude approximation but we try to keep the number of free parameters in our model as low as possible.

Furthermore, we take the chemical and optical properties of the considered dust material to be invariant with respect to changes of both temperature and density (see Henning & Mutschke in prep. for a more detailed discussion).

4.4. Coagulation

In this paper, we concentrate on the coagulation process (see also Appendix). This process can be described by a simple "chemical" reaction

$$Y(V') + Y(V'') \rightarrow Y(V' + V''),$$

and its mathematical formulation is represented by the Smoluchowski equation

$$\frac{\partial}{\partial t} f(\boldsymbol{r}, t, V) = S_{\rm cgn}, \tag{51}$$

where $S_{\rm cgn}$ will be given by the Eq. (A1) in the Appendix. Here, we have neglected other processes (omitted transport terms on the l.h.s. of the Eq. (13) and other source terms on the r.h.s. of the equation) corresponding to a local treatment of the coagulation. We adopt this approach for the numerical calculations presented in the following. The coagulation kernel $R_{\rm cgn}$ describing the probability of a cohesive collision of two grains is given by

$$R_{\rm cgn} = \sigma(V_1, V_2)\, v_{\rm rel}(\boldsymbol{r}, t, V_1, V_2)\, S(V_1, V_2), \tag{52}$$

where $v_{\rm rel}$ and S are the relative velocity between the particles and the sticking efficiency during the collision, respectively. The sticking efficiency for small particles (μm-sized) is practically one (Blum et al. 1996). For larger particles (above μm-sized) this function is rather unknown, although calculations concerning collisions of small compact spheres by Chokshi et al. (1993) and experimental work by Blum & Münch (1993) give some restrictions on S. We use a value $S = 1$ for most of our local calculations because the critical velocities given by these authors are practically never reached (see also Sect. A.2.1). The relative velocity $v_{\rm rel}$ of the dust grains is given by Eqs. (42-46). The effective collisional cross section σ is determined according to the fractal properties of our fluffy grains (Ossenkopf 1993).

4.5. Numerical method

The adequate numerical solution of a partial integrodifferential equation remains a different task. We developed a new method (Mucha in prep.) which we call adaptive binning. Using the so-called Rothe algorithm we first discretized the time dependence. This results in a sequence of stationary problems. Both in physical and in volume (mass) space, we divide the integration domain into intervals which are refined or roughened adaptively during the calculation. The dust distribution function f is decomposed in spectral modes (Deulfhart & Wulkow 1989) using appropriate basis functions. The expansion is adaptively truncated after a few terms in order to save computation time. The truncation error is controlled during the whole computation. For the time integration, we use a two-level adaptive time stepping explicit algorithm for the "pure" coagulation and a semi-implicit method (Deulfhart 1985) for more complex problems.

We tested the algorithm against the known analytical solutions for bilinear coagulation kernels. The achieved accuracy was always below 10% in relative error. Actually, it was much better but a 10% error was approached at the very beginning and at the end of the time integration. Mass (volume) conservation in coagulation was guaranteed.

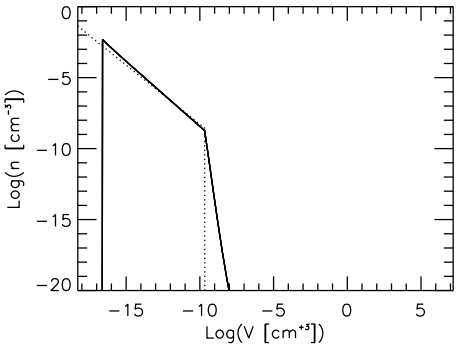

Fig. 1. Size distribution of CCA dust grains after 100 yrs (solid line) at a disk radius of 40 AU starting with a MRN distribution (dotted line)

5. Results and discussion

5.1. Coagulation

For CCA-like dust particles, there is no growth after the disappearance of the smallest grains (see Fig. 1). This is an expected outcome because the CCA particles have vanishingly small relative velocities. The smallest particles consisting of about up to 25 members behave like PCA's (see Ossenkopf 1993) and thus consequently, they have the same starting phase of their evolution. This is a reason for their fast vanishing.

Although we believe that a growth mode between CCA and PCA is more realistic – even if not sufficiently theoretically and experimentally proved until now (Blum et al. 1996) –, we especially focus on the PCA growth in order to study this extreme case, its rapid coagulation, and its effects to the accretion disk in a reasonable computational time. Thus, we avoid an extensive and arbitrary parameterizations (Ossenkopf 1993, Weidenschilling 1997) as well as numerous parameter studies. Additionally, the compact PCA aggregates are considerably well approximated by the used effective medium theory (see Sect. 4.3).

For the PCA dust particles, we find three characteristic evolutionary stages during the coagulation:

1. *Starting phase*: The first phase of the coagulation is characterized by the fast disappearance of the smallest particles. The total mass (volume) is spread over a relatively small particle size interval (see Fig. 2).
2. *Phase of self-similar growth*: During the second evolutionary stage a significant part of the distribution can be described by scaling laws (see Fig. 3). The self-similar parts in the dust distribution become larger as the coagulation proceeds. The total mass is dispersed slightly more than in the first phase.
3. *Transition phase*: In the last phase of the evolution, a wide part of the distribution shows a scaling behaviour (see Fig. 3). The most massive particles begin to decouple from

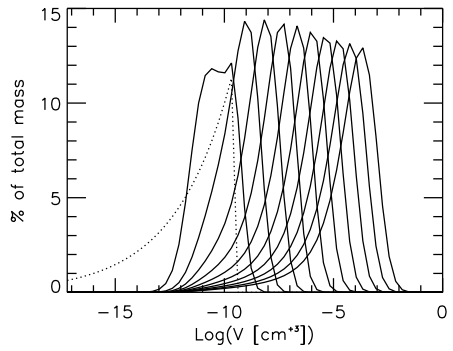

Fig. 2. Evolution of the relative mass fraction in particular sizes of the PCA dust grains after a period of 10, 20, . . ., 100 yrs at a radius of 30 AU starting with a MRN distribution (dotted line)

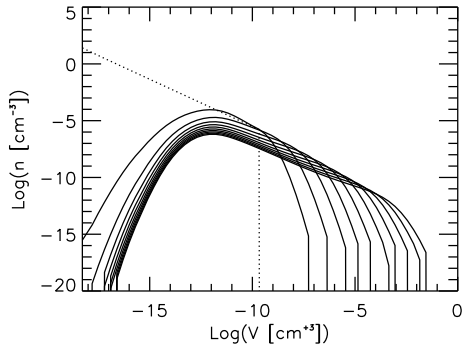

Fig. 3. Same as Fig. 2, but for the size distribution of PCA dust grains

the gas motion, and drift motions become an important source of relative velocities. The approximation we adopted breaks down here. However, this does not cause any problems in the simulations because the part of the distribution containing relatively small grains remains preserved during the timescales considered. Furthermore, the larger grains do not significantly contribute to the dust opacity.

The radial dependence of the dust distribution functions shows a more rapid growth of particles in the inner regions of the disk (Fig. 4). Crucial gas parameters influencing the coagulation timescale are the density and the temperature (see also Eqs. (43), (16), and (44-46)) because they determine the relative velocity between the dust grains and they increase towards the inner parts of the disk.

In the first evolutionary stage where the "Brownian" velocities are the largest velocities, the coagulation rate does not explicitly depend on the gas density (Eq. (43)). This is nicely demonstrated by the fact that the smallest particles rapidly vanish. Their relative velocities are dominantly produced by Brownian (thermal) motion. Thermal motion "prefers" collisions of the smallest particles of the same size with a rate depending only on the local temperature (see Eq. (42)). Consequently, this growth regime narrows the initial mass distribution, thus reducing the effect of the shape of the initial distribution on

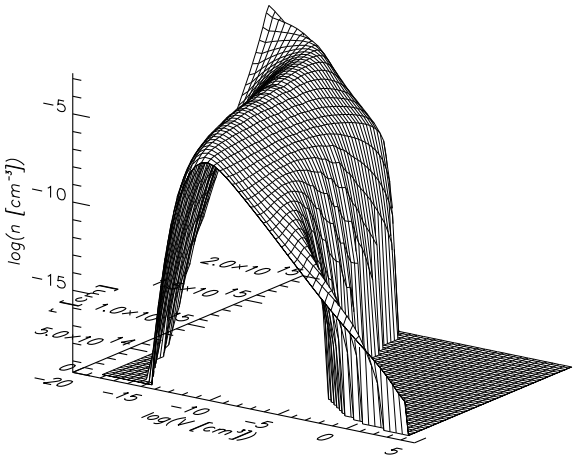

Fig. 4. Size distributions of dust grains after a period of about 100 yrs at different radii of the protoplanetary accretion disk

the further evolution (see also below). Brownian motion-driven coagulation moves the particle sizes to the region where the turbulence-induced velocities between grains become the dominating factor for the growth process. The first aggregates gaining turbulence-induced relative velocities are sweeping out the smaller grains, which accelerates the reduction of the relatively abundant small grains. At the time of the onset of the turbulent coagulation regime a double-peaked distribution of the relative mass concentration around particular grain sizes occurs (Fig. 3). This threshold is the beginning of the second evolutionary phase (period of self-similar growth).

In the turbulent regime (relative velocities mainly produced by turbulence) the dependence of the coagulation kernel on temperature and density becomes more complicated

$$\langle \Delta v_{12}^2 \rangle \approx \sqrt{\rho_g\, T}\, \sqrt{1-\rho_g} \sim \sqrt{\rho_g\, T}, \quad (\rho_g \ll 1). \tag{53}$$

The explicit density dependence is introduced by the friction time τ_f only and the temperature dependence by the parameterization of the turbulence ($v_{\rm turb} = \alpha^{1/2}\, c_s$). Relative turbulent velocities slowly decrease with growing V/A ratios. For PCA particles this ratio increases with the growth of the compact volume and thus it is also a measure of the particle size. This favors the growth of the small particles in the vicinity of the threshold size. Grains of other sizes are sweeping out the small particles, which is broadening the size distribution. This self-similar growth can be seen in Fig. 3. The relative fast transition from the Brownian to the turbulent growth regime result in the subsequent exhausting of the reservoir of the actually smallest particles. The broadening of the distribution induces a decrease of the number density of particles at all sizes consequently dispersing the total mass more "homogeneously", i.e., on the slightly larger interval around the dominating particle size (see Fig. 2). The broadening of the size distribution is reflected by the evolution of the opacity. The absolute values of the Rosseland mean opacity drop (see Fig. 5) and the opacity becomes a weaker function of the temperature. We stress that even at the start of the dust

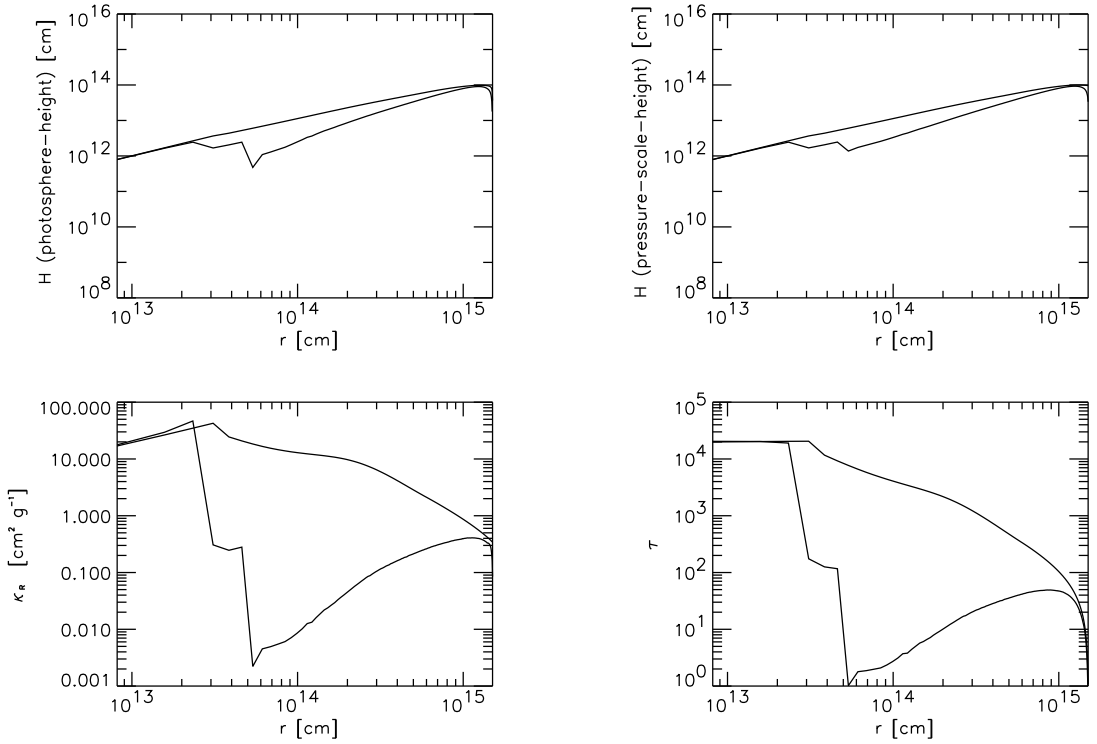

Fig. 5. Photosphere height (*top left*), pressure scale height (*top right*), Rosseland mean opacity (*bottom left*), and optical depth (*bottom right*) of the disk at the beginning (upper curve) and after 100 yrs (lower curve) at different radii of the protoplanetary accretion disk

disk evolution, there is never a square power dependency of the Rosseland mean opacity on the temperature. This was until now a common assumption of any simulation of disks containing a dust component and, furthermore, this dependency was taken to be stationary (see, e.g., Ruden & Pollack 1991). However, the spectral appearance of the accretion disk does not change as dramatically as the dust population and the opacities. The reason for this behaviour is quite simple. The outer disk regions of lower density and, consequently, of slow coagulation dominate the luminosity of the whole dusty part of the disk. They give the lower frequency part of the spectral luminosity curve.

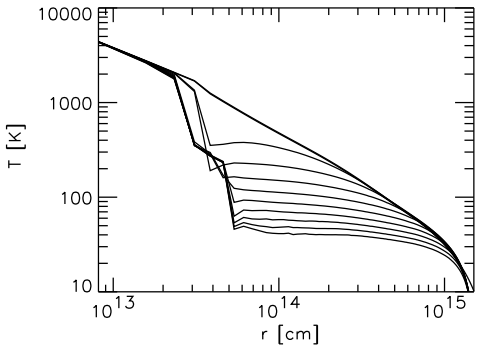

Fig. 6. Evolution of the central temperature of the protoplanetary accretion disk after a period of 10, 20, . . ., 100 yrs (from top to bottom)

Because coagulation proceeds faster in the inner regions of the disk, an interesting gap in its thermal structure evolves at the very frontier of the coagulation zone (Figs. 5-6). The "thermal gap" position remains relatively insensitive to the total number of grid points and to the iteration criteria applied (the overall shape of the gap varies a little). Our analysis suggest that the oscillatory behaviour is induced by large gradients between neighboring points in the gap region, which generate a local peak. This is then transported by the solver as a damped numerical wave. The natural damping by the large turbulent disk viscosity is unfortunately not able to suppress the oscillations just on their very beginning. The time integrator may also play its role. The depth of the gap may be significantly affected (see also below) by our assumptions that after the temperature in the former dust-free regions had dropped below the critical dust "destruction" value ($T_{\rm crit} = 1500K$) an initial distribution of the MRN-shape immediately establishes and that the dust-to-gas ratio in the whole dusty part of the disk is the same. Since the region at this threshold is relatively dense, the initial distribution contains a large amount of small particles making the transition phase from Brownian to the turbulent regime very efficient (also the both regimes themselves) thus resulting in a significant drop in the absolute value of the opacity (in this transition phase, the numerical time integration of the disk can introduce an error comparable with the spatial one). Despite the numerical problems, the gap seems to be a physical feature induced by the coagulation of the grains supported by the slow diffusion whose timescale is inversely proportional to the

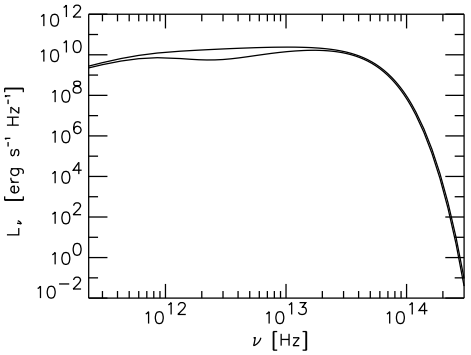

Fig. 7. Spectral luminosity of the entire accretion disk L_ν at the beginning (upper curve) and after 100 yrs of coagulation (lower curve)

viscosity which by itself is a linear function of the central temperature. The effect of establishing a "thermal gap" and of the coagulation as a whole on the spectral luminosity is in "digging a shallow hole" in the intermediate frequency region (Fig. 7). The coagulation mainly broadens the outer cool region hence inducing the growth of the cold low-frequency hump. The influence of the "thermal gap" region is rather minor because of its small extent compared to the outer parts and its low temperature compared to the neighboring hottest parts of the disk. Here, we recall that the luminosity is given by the surface temperature of the disk which does not change as much as the central one. The central temperature drops as a consequence of the lowered opacity but at the same time the optical depth also decreases for the same reason. These two changes cancel out each other to a large amount leaving the surface temperature more "stable" than the central one. The effect is a slight deepening of the "luminosity hole". This feature is not strongly pronounced and we expect it to be only a relatively short lasting "adventure" in the overall evolutionary history of the disk.

When the particles have grown as large as $V \sim 1\text{cm}^3$, conceptual difficulties related to the breakdown of some of the assumptions and of the Smoluchowski equation itself appear. Analytical studies of the coagulation equation for bilinear kernels ($R_{\text{cgn}}(V, V') \sim 1$, $V + V'$, and $V \times V'$) suggest that the equation in its mean field statistical form describes the coagulation process only until the particles have reached a particular limiting size (Tanaka & Nakazawa 1994). From the comparison of the discrete coagulation equation with the results obtained for the master equation describing the discrete coagulation, the validity of the Smoluchovski equation seems to be granted until the coagulating bodies have grown approximately to the mass comparable to the total mass. After reaching this critical value the runaway growth of the largest bodies sets in. This behaviour is also shown by numerical simulations (Ohtsuki et al. 1990; Wetherill 1990). This stage also appears in our calculations at the time when the largest particles become much larger as $V \sim 1\text{cm}^3$. This is indicated by the slowing down of the growth of the largest particles. This does not mean that no larger grains exist but only that the amount of that grains is very small compared to the smaller ones. This is not longer resolvable by the statistical approach. However, we cannot simply ignore the fact that the particles larger than $V \sim 1\text{cm}^3$ are aggregates consisting of billions of smaller grains. The structure of such particles is unknown. The assumption that they are still PCA particles seems not to be appropriate anymore. For the largest grains, there is also a change in their aerodynamical properties. They switch from the Knudsen free molecular interaction regime to the Stokes hydrodynamical interaction regime with the surrounding gas (see Eqs. (16) and (17)). For the reasons we mentioned, we cut the distribution where the transition phase occurs. This does not influence the distribution of smaller grains and, consequently, the opacities does not change much (the largest grains are in the limit of geometrical optics and their contribution to the extinction is negligible) and thus the accretion disk itself is also not immediately influenced by the onset of the transition phase of the growth. However, if we take sedimentation into account, the dust evolution would be influenced significantly by the largest bodies colliding with smaller ones while traveling towards the disk midplane. To understand this process better, a detailed modelling of the dust distribution evolution by the means of the stochastic coagulation equation or of the corresponding master equation would be necessary (see also Sect. 4).

5.2. Some important factors influencing the dust evolution

So far, we mainly restricted our discussion to the analysis of the local coagulation in the disk. Now, we will give some estimates concerning possible influences due to other evolutionary processes we mentioned earlier (see also Appendix). We will also consider the possible effects of the non-locality.

5.2.1. Effects of the advection and the diffusion

The grains are transported through the nebula in two different ways, namely by advection and diffusion (see Eqs. (13) and (29)). The first of these transport mechanisms is a deterministic one which is due to the mean dust velocity $\boldsymbol{v}_d$ (see Sect. 4.2). The second one is of stochastic nature and is induced by the Brownian (thermal) v_{dB} and turbulent velocity $\boldsymbol{v}'_d$ (see Sects. 4.2 and 4.4). Rewriting the evolutionary Eq. (29) with a single source term given by the coagulation in cylindrical coordinates and omitting the characteristic timescales of the respective terms, we get

$$\frac{\partial f(\varrho,\tau,V)}{\partial \tau} + \frac{\epsilon_{\text{adv}}}{\varrho}\,\frac{\partial}{\partial \varrho}\left(\varrho\, w_{dr}(\varrho,\tau,V)\, f(\varrho,\tau,V)\right) - \frac{\epsilon_{\text{dif}}}{\varrho}\,\frac{\partial}{\partial \varrho}\left(\varrho\, D(\varrho,\tau,V)\,\frac{\partial}{\partial \varrho} f(\varrho,\tau,V)\right) = \epsilon_{\text{coa}}\,\left(F_{\text{gain}} - f(\varrho,\tau,V)\right), \tag{54}$$

where the non-dimensional similarity numbers are given by

$$\epsilon_{\text{index}} = \left(\frac{\tau_{\text{index}}}{\tau_{\text{adv}} + \tau_{\text{dif}} + \tau_{\text{coa}}}\right)^{-1} \tag{55}$$

with the characteristic times defined as

$$\tau_{\rm adv} = \frac{R}{V_{dr}}, \qquad \tau_{\rm dif} = \frac{R^2}{D^*},$$
$$\tau_{\rm coa}^{-1} = \int R_{\rm cgn}(\boldsymbol{r}, t, V, V')\, f(\boldsymbol{r}, t, V')\, dV' \tag{56}$$

and $F_{\rm gain}$

$$F_{\rm gain} = \frac{\tau_{\rm coa}}{2} \int\int R_{\rm cgn}(\boldsymbol{r}, t, V', V'')\, f(\boldsymbol{r}, t, V')\, f(\boldsymbol{r}, t, V'') \times \delta(V - (V' + V''))\, dV' dV''. \tag{57}$$

The r.h.s. of Eq. (54) resembles the so-called BGK form of a kinetic equation (see, e.g., Landau et al. 1988). The differential operators were also transformed in non-dimensional operators with τ, ϱ being the non-dimensional time and the non-dimensional radial coordinate, respectively. The set of non-dimensional quantities is completed by the mean radial velocity w_{dr} and the simple scalar diffusion constant D (see also Sect. 4.2). The reference values are the typical radius R, the typical radial velocity V_{dr} and the typical diffusion constant D^*; those are the disk radius, the maximum radial velocity at the initial time, and the turbulent viscosity ν. Since turbulent viscosity is the limiting maximal diffusion constant which is approached by smallest particles, it leads to an underestimate of the diffusion timescale, i.e., to overestimating the order of the diffusion term. The characteristic times $\tau_{\rm adv}$ and $\tau_{\rm dif}$ approximate reasonably well the timescales for advection and diffusion which are given by

$$\frac{1}{\tau_{\rm adv}} = \frac{1}{r}\frac{\partial}{\partial r}\left(r\, v_{dr}(r, t, V)\, f(r, t, V)\right) \frac{1}{f(r, t, V)} \tag{58}$$

and

$$\frac{1}{\tau_{\rm dif}} = \frac{1}{r}\frac{\partial}{\partial r}\left(r\, D(r, t, V)\, \frac{\partial}{\partial r} f(r, t, V)\right) \frac{1}{f(r, t, V)}. \tag{59}$$

For the computation of the timescales, we used the initial MRN distribution because it provides the shortest timescales. The comparison of the timescales shows that in the most parts of the dust disk the advection and diffusion timescales are much larger compared to the coagulation timescale and also larger than the timescale (about 10^2 yrs) we followed in our computations (see Fig. 8). Consequently, our local treatment of the coagulation seems to be justified as an approximation of lowest order (in $\epsilon_{\rm coa}$). However, we did not consider the settling timescale. This timescale can be of the order of the coagulation timescale. As a consequence, we may state once more that the settling could have an important influence on the evolution of the grains (see also Weidenschilling 1980), whereas we expect that it rather speeds up the growth of the dust particles. More detailed, combined radial and vertical calculations, utilizing the full Eq. (13) are in progress.

5.2.2. Initial dust distribution function

In order to clarify the influence of the initial distribution, we performed calculations for power law distributions of different non-positive powers. The influence of the shape of the initial distribution seems to be relatively unimportant, resulting in a slight slowing down for shallower distributions, i.e., distributions containing a lower amount of small particles (see also Sect. 5.1). Distributions of more complicated shape were not investigated in this paper. The intrinsic nonlinearity of the dust evolution equation would suggest that the modelled system could be relatively sensitive on initial conditions and that a complicated topology of the phase space should be expected. Further investigations on this topic are needed.

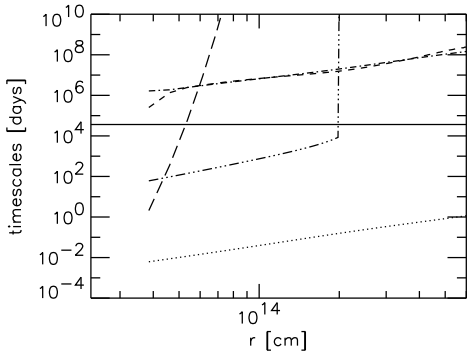

Fig. 8. Comparison of timescales relevant for the evolution of dust in the disk. Coagulation timescale $\max_V \tau_{\rm coa}(V)$ (dotted line), advection timescale $\min_V \tau_{\rm adv}(V)$ (dash-dot line), diffusion timescale $\min_V \tau_{\rm adv}(V)$ (short dashed line), collisional destruction timescale $\min_V \tau_{\rm cdn}(V)$ (dash-dot-dot line) and timescale for sublimation, condensation and chemical destruction $\min_V \tau_{\rm ecs}(V)$ (long dashed line). The time of 100 yrs is given by the solid line

6. Conclusions

We investigated the dust coagulation in protoplanetary accretion disks – for the first time, by coupling the disk and dust evolution in a time-dependent, numerical model. It was demonstrated that variations of the dust opacity cause changes in the energetic structure of the disk. For the coagulation of PCA particles, our results show three characteristic evolutionary stages: a initial (Browninan) phase, a phase of "self-similar" growth, and a transition phase. In the case of particles grown by CCA, however, we found no dust growth after disappearance of the smallest grains. The different characteristical times for the coagulation at different radii result in the restructuring of the dust region of the protoplanetary disks: Due to faster growth of the dust grains in the inner part of the disk, the opacity drops faster here. As a consequence, a "gap" in thermal and optical characteristics of the accretion disk appears at the very frontier of the coagulation, i.e., behind the sublimation boundary in the region between 1 and 5 AU and the spectral luminosity curve shows a shallow double hump feature.

Acknowledgements. We would like to thank K. Robbins Bell, Willi Kley, Volker Ossenkopf, and Michael F. Sterzik for valuable discussions and helpful hints. The research for this paper was partly supported

by DFG grant He 1935/4-1 within the special programme "Physics of Star Formation".

Appendix A: processes involved in the evolution of dust grains

A.1. Mathematical formulation

From the processes involved in the evolution of dust grain ensemble, we pick up the following 7 ones:

$$
\begin{aligned}
&S_{\rm cgn} = \\
&\quad -f(\boldsymbol{r},t,V)\int dV'\, f(\boldsymbol{r},t,V')\, R_{\rm cgn}(\boldsymbol{r},t,V,V') \\
&\quad +\frac{1}{2}\int\int dV'dV''\, f(\boldsymbol{r},t,V')\, f(\boldsymbol{r},t,V'') \\
&\quad \times R_{\rm cgn}(\boldsymbol{r},t,V',V'')\,\delta(V-(V'+V'')) \qquad \text{(A1)}
\end{aligned}
$$

takes into consideration coagulation by the collisions of the dust particles.

$$
\begin{aligned}
&S_{\rm cdn} = \\
&\quad -f(\boldsymbol{r},t,V)\int dV'\, f(\boldsymbol{r},t,V')\, R_{\rm cdn}(\boldsymbol{r},t,V,V') \\
&\quad +\frac{1}{2}\int\int\int dV'dV''dV'''\, f(\boldsymbol{r},t,V')\, f(\boldsymbol{r},t,V'') \\
&\quad \times F(V,V''')\, R_{\rm cdn}(\boldsymbol{r},t,V',V'')\,\delta\big(V'''-\big(V'+V''\big)\big) \qquad \text{(A2)}
\end{aligned}
$$

accounts for the effects of collisional destruction of the dust.

$$
\begin{aligned}
&S_{\rm acc} + S_{\rm scn} + S_{\rm chd} \equiv S_{\rm ascd} = \\
&\quad -\sum_a f(\boldsymbol{r},t,V)\, g(\boldsymbol{r},t,V^a_{\rm mol})\, R_{\rm acc}(\boldsymbol{r},t,V^a_{\rm mol},V) \\
&\quad +\sum_a \int dV' f(\boldsymbol{r},t,V')\, g(\boldsymbol{r},t,V^a_{\rm mol}) \\
&\quad \times R_{\rm acc}(\boldsymbol{r},t,V^a_{\rm mol},V')\,\delta(V-(V'+V^a_{\rm mol})) \\
&\quad -\sum_i f(\boldsymbol{r},t,V)\, R_{\rm scn}(\boldsymbol{r},t,V_i,V) \\
&\quad +\sum_i \int dV' f(\boldsymbol{r},t,V')\, R_{\rm scn}(\boldsymbol{r},t,V_i,V') \\
&\quad \times\delta(V-\Gamma_{\rm scn}(V',V_i)) \\
&\quad -\sum_b\sum_i f(\boldsymbol{r},t,V)\, g(\boldsymbol{r},t,V^b_{\rm mol}) \\
&\quad \times R_{\rm chd}(\boldsymbol{r},t,V^b_{\rm mol},V_i,V) \\
&\quad +\sum_b\sum_i \int dV' f(\boldsymbol{r},t,V')\, g(\boldsymbol{r},t,V^b_{\rm mol}) \\
&\quad \times R_{\rm chd}(\boldsymbol{r},t,V^b_{\rm mol},V_i,V')\,\delta(V-\Gamma_{\rm chd}(V',V^b_{\rm mol},V_i)) \qquad \text{(A3)}
\end{aligned}
$$

describes possible jump-like changes in the mass of the dust particles due to the accretion of molecules onto preexisting grains, sublimation/condensation and chemical destruction.
Finally,

$$S_{\rm acr} = Q_{\rm acr}(\boldsymbol{r},t,V) \qquad \text{(A4)}$$

gives the supply of the grains by the accretion from the remaining cloud surrounding the protoplanetary disk. Eqs. (A1-A3) describe discontinuous, jump-like changes of the compact volume of grains. Here, $R_{\rm proces}$ are the interaction rates, $\Gamma_{\rm proces}$ describe the volume (mass) conservation in the interactions, the indices mark different types of molecules, and $g(\boldsymbol{r},t,V^{\rm index}_{\rm mol})$ stands for the number densities of molecules of type $index$. Furthermore, $F(V,V')$ is the distribution function of the fragments after a collision of two particles with a total volume V'. In Eq. (A4), $Q_{\rm acr}(\boldsymbol{r},t,V)$ is the accretion rate for the particles of size V from outside of the disk. In Eq. (14), $W_{\rm proces}$ is the rate of continuous change of the compact volume of a dust particle due to the corresponding physical process, i.e., accretion of the molecules on the surface of the grain, sublimation/condensation and chemical destruction. We introduced a common index for the processes in order to keep formulas as simple as possible.

A.2. Processes apart from coagulation

In the following sections, we briefly describe the remaining six processes (apart from coagulation) we mentioned in Sect. 4.1 and Appendix A.1.

A.2.1. Collisional destruction

At the present time, only one experimental study on the aggregate-aggregate collisions under the conditions of an early protoplanetary nebula by Blum & Münch (1993) (BM) is available. Their $ZrSiO_4$ particles seem to be an acceptable analogy of our PCA's. The onset of fragmentation was observed for collision velocities of about 1 ms^{-1}. Below this critical velocity, the particles were bouncing off after the impact without measurable mass loss or mass transfer. Significant fragmentation occurred only for particles of similar sizes of about 1 mm. Destruction of the grains in collisions can be described by the following "chemical" reaction

$$Y(V') + Y(V'') \rightarrow \textstyle\sum_\alpha M_\alpha\, Y(V_\alpha),$$

and its mathematical formulation is represented by the Smoluchowski-like equation with the source term $S_{\rm cdn}$ given by Eq. (A2). The interaction coefficient $R_{\rm cdn}$ describing the probability of a destructive collision of two grains is expressed by

$$R_{\rm cdn} = \sigma(V_1,V_2)\, v_{rel}(\boldsymbol{r},t,V_1,V_2)\, D(\boldsymbol{r},t,V_1,V_2), \qquad \text{(A5)}$$

where $v_{\rm rel}$ and D are the relative velocity between particles and the fragmentation efficiency of the collision, respectively. Assuming Kolmgoroff-like scaling of the fragment distribution function $F(V,V''') = K(V)\,\left(V'''\right)^k\, dV$, BM's Eqs. (25-26) expressing specific surface enhancement energy in terms of the power law fragment mass distribution can be used to determine the power law exponent k.

An appropriate timescale for the estimates of importance of the collisional destruction can be obtained by transforming Eq.

(A2) into the BGK-like form. We yield

$$
\begin{aligned}
S_{\rm cdn} &= \frac{G_{\rm gain} - f(\varrho,\tau,V)}{\tau_{\rm cdn}},\\
G_{\rm gain} &= \frac{\tau_{\rm cdn}}{2}\int\int\int dV'dV''dV'''f(\boldsymbol{r},t,V')\,f(\boldsymbol{r},t,V'')\\
&\quad\times F(V,V''')\,R_{\rm cdn}(\boldsymbol{r},t,V',V'')\,\delta\big(V'''-\big(V'+V''\big)\big),\\
\tau_{\rm cdn}^{-1} &= \int R_{\rm cdn}(\boldsymbol{r},t,V,V')\,f(\boldsymbol{r},t,V')\,dV', \qquad \text{(A6)}
\end{aligned}
$$

where $R_{\rm cdn}$ is given in Eq. (A5) and G_{gain} being the mean gain term due to the destructive collisions. The corresponding timescales are plotted in Fig. (8). The fragmentation efficiency D was taken to be $D = 0$ for $v < v_{\rm sticking}$ and $D = 1$ otherwise, where $v_{\rm sticking}$ is the sticking velocity taken from Chokshi et al. (1993). This assumption leads to overestimating of the importance of the destructive collisions. The critical velocity measured by BM is much higher. Recent experimental results of Wurm et al. (in prep.) also show sticking at the velocities well above $v_{\rm sticking}$ of Chokshi et al. (1993). For the calculation of the timescales, the MRN distribution was used.

A.2.2. Accretion of molecules onto preexisting grain

We restrict ourselves only to a particular accretion process we call accretion of "dirty" ice mantles. This process can be described as the "chemical" reaction

$$X(V^a_{\rm mol}) + Y(V') \rightarrow Y(V' + V^a_{\rm mol}).$$

It is mathematically expressed in the first two terms of Eq. (A3) where $R_{\rm acc}$ is determined by the projected area of the dust particles and the relative velocity between the gas molecules and the grain. In general, the sticking efficiency $S_{\rm ice}$ is a function of local physical conditions and it is also radial and time dependent. For ice, however, the sticking efficiency is practically 1. Following the approach of Ossenkopf (1993) one can assume:

1. The accretion process is represented by the accretion of one type of "averaged" molecules. However, we allow for the changes in chemical composition of these molecules depending on the local environment they are "living" in.
2. The growth is compact, i.e., the mantle layers are homogeneous and of low density and the fractal properties of the accreting grains are not changed.

We replace Eq. (A3) in accordance with Sect. 4.1 for grains large enough to be concerned as continuum by

$$W_{\rm acc} = g(\boldsymbol{r},t,V^a_{\rm mol})\,R_{\rm acc}(\boldsymbol{r},t,V^a_{\rm mol},V). \qquad \text{(A7)}$$

This equation is more convenient than Eq. (A3).

A.2.3. Sublimation, condensation and chemical destruction

Although all processes described in this section are due to interaction of gas atoms and molecules with the dust grains, we model them in different ways. The sublimation and condensation are treated as thermodynamical processes, i.e., as an interaction of the particle with a field characterized by its state variables, mainly temperature. This can be described by a single "chemical" reaction

$$Y(V') \rightarrow Y(V).$$

On the other side the erosion of the dust grains is treated as gas-dust particle interaction represented by

$$X(V^b_{\rm mol}) + Y(V') \rightarrow X(V^b_{\rm mol}) + Y(V).$$

The mathematical form for the sublimation and condensation and for the destruction is given by second two and last two terms of Eq. (A3), respectively. In accordance with 4.1, we understand the mass (volume) changes as continuous ones in the limit $V \gg V_i$. The condensation, sublimation, and rate of chemical destruction $W_{\rm ecs} \equiv W_{\rm scn} + W_{\rm chd}$ is given (Gail & Sedlmayr 1988, Lenzuni et al. 1995 and Duschl et al. 1995) for fluffy grains by

$$W_{\rm ecs} = 4\,A(V)\,J_{\rm ecs}(V,T,\rho), \qquad \text{(A8)}$$

where $A(V)$ is the cross section of the grain and $J_{\rm ecs} = J_{\rm scn} + J_{\rm chd}$ the rate of the interaction given by

$$J_{\rm scn} = \sum_i \sum_j \left(J^a_{\rm scn(ij)} - J^d_{\rm scn(ij)}\right),$$

$$J_{\rm chd} = -\sum_i \sum_j J^d_{\rm chd(ij)}.$$

The quantities $J^a_{(ij)}$ and $J^d_{(ij)}$ are the rate of addition and decomposition of the material i (silicate and carbon) due to interaction with molecule j, respectively. They are of following shape

$$J^a_{\rm scn(ij)} = S_{ij}\,V_{0j}\,v^{\rm th}_j\,\frac{P_j}{kT},$$

$$J^d_{\rm scn(ij)} = S_{ij}\,V_{0j}\,v^{\rm th}_j\,\frac{P^s_j}{kT},$$

$$J^d_{\rm chd(ij)} = Y_{ij}\,V_{0j}\,v^{\rm th}_j\,g_j,$$

where S_{ij} is the "sticking probability" for molecule j hitting material i, V_{0j} is the specific volume occupied by the nominal molecule of solid in the condensate, $v^{\rm th}_j$ is the thermal velocity of the molecule j, g_j is the number density of molecule j and Y_{ij} is the yield of chemical destruction (sputtering) due to molecule j. The quantities P^s_j, P_j are the partial pressure in chemical equilibrium and the partial pressure of j, respectively. In order to evaluate Eq. A8, we make use of the model developed by Lenzuni et al. (1995) and Duschl et al. (1995). We took the chemical sputtering by hydrogen into account (Lenzuni et al. 1995), thus probably overestimating the destruction rate of carbon (Duschl et al. (1995)). For the sake of simplicity, the transport of vapour was ignored which corresponds to the assumption that the radial transport of vaporized material does not play a significant role on the timescales we considered.

As we stated earlier, we mainly restricted ourselves to the "pure" coagulation in this work. Nevertheless, we have implicitly included the condensation in a crude manner by the assumption on the immediate establishing of a MRN distribution after the temperature dropped below the critical value. The influence of this assumption can not be considered to be small and its admissibility has to be checked (but we do not expect that the main result, i.e., appearance of a thermal "gap" will be changed), in contrast to the previous Sects., where we could argue that some of the discussed effects can be understood as a kind of higher order correction to the coagulation. In a first case, we took the opacity given by molecules (from Bell & Lin 1994), i.e., we assume no dust there. In a second case, we assumed that there is a small amount of dust grains given by the MRN distribution for a low density medium ($n = 10^5\ cm^{-3}$). The results of that procedure are shown in Fig. 9. One can see that the disk becomes transparent at the point where the temperature drops below the critical value $T = 1500K$. The approximation of a optically thick disk breaks down here. Thus, the assumption of the immediate establishing of a MRN distribution leads to underestimating the effect of the temperature drop. Now, we consider the timescales as determined by the Eq. (A8). An appropriate timescale is given by $\frac{1}{\tau_{\rm ecs}} = \frac{\partial}{\partial V}\left(\dot{V} f(V)\right) \frac{1}{f(V)} \{\approx \frac{W_{\rm ecs}}{V}\}$. The comparison of the timescales shows that in the most parts of the dust disk the timescale defined above is much larger compared to the coagulation timescale and also larger than the timescale (about 10^2 yrs) we followed in our computations (see Fig. 8). For the computation of the timescales, we used the initial MRN distribution because it provides the shortest timescales.

A.2.4 Accretion of dust from the collapsing cloud

The accretion of dust from the rest of the collapsing cloud onto the protoplanetary disk can be described by the following "chemical" reaction

$$Y(V) \rightarrow (M+1)Y(V),$$

and its mathematical form is given by Eq. (A4). The source term $Q_{\rm acr}$ can be estimated as

$$Q_{\rm acr}(\boldsymbol{r}, t, V) =$$

$$f_{\rm acr}(\boldsymbol{r}, t, V)\, \xi_d(\boldsymbol{r}, t, V)\, \dot{\Sigma}_{\rm acr}(\boldsymbol{r}, t)/\Sigma_{\rm dust}(\boldsymbol{r}, t), \qquad \text{(A9)}$$

where $f_{\rm acr}$ and ξ denote the accreted dust distribution and the dust abundance, respectively. The rate of gaining surface density due to infall is described by $\dot{\Sigma}_{\rm acr}$ and $\Sigma_{\rm dust} = \rho^{\rm acr}_{\rm dust} 2H$, $\rho^{\rm acr}_{dust}$ being the accreted dust density. As an approximation for $f_{\rm acr}$, we use the MRN distribution. The dust to gas ratio is considered to be constant (about 0.01). Our disk model represents the evolutionary stage where the collapse is already finished up to some remnant which do not influence the disk itself. The flow of matter onto the disk is hypersonic and the streamlines of the fluid are parabolas as long as the rotational energy of the gas is small (Cassen & Pettibone 1976) and no very strong magnetic fields are involved. Both conditions mentioned above seem to be granted. Consequently, the gain of the surface density due to the accretion from the surrounding region is given by (Cassen & Moosman 1981)

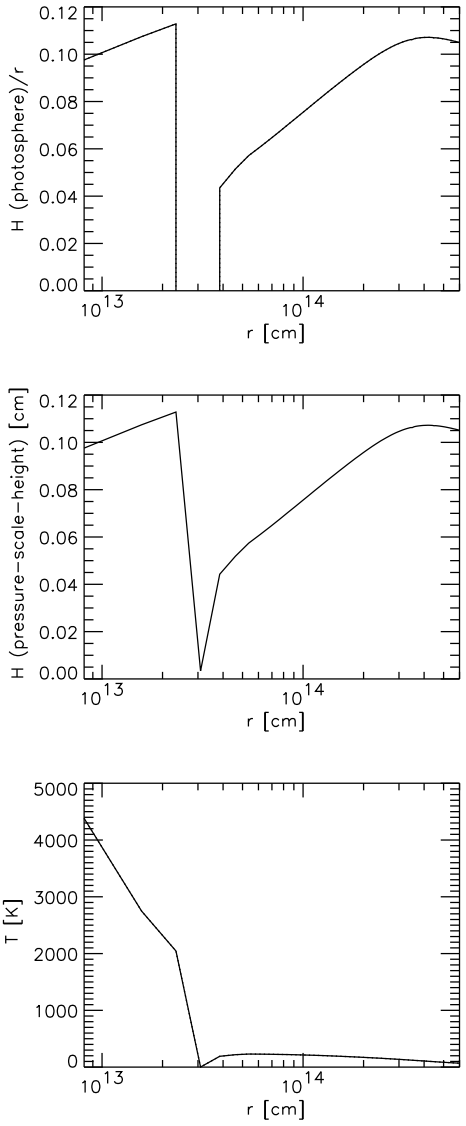

Fig. 9. Photosphere height (*top*), pressure scale height (*center*), and central temperature (*bottom*) of the disk after 20 yrs without immediate establishing of a MRN distribution after the temperature dropped below the critical value $T = 1500K$. Curves representing no dust at all and a very small amount of grains do not differ on this plotting scale

$$\dot{\Sigma}_{\rm acr} = \frac{\dot{M}_{\rm acr}}{\pi\, r^2_{\rm disk}} \frac{\left(1-u^{0.5}\right)(3-2u)}{4u\ (1-u)^{1.5}} \qquad \text{(A10)}$$

for $u < 1$ and

$$\dot{\Sigma}_{\rm acr} = 0 \qquad \text{(A11)}$$

for $u > 1$, where $u = r/r_{\rm disk}$. The accretion rate for the remnant of the collapsed cloud $\dot{M}_{\rm acr}$ is taken to be a free parameter which has to be supplied according to the particular model.

In the whole disk the accretion timescale remains well above the coagulation timescale and also above the timescale considered ($\approx 100yrs$) for $\dot{M}_{\rm acr} \lesssim 10^{-6} M_\odot\ yr^{-1}$. The maximal value for $\dot{M}_{\rm acr}$ equals our adopted radial accretion rate ($\dot{M}_{\rm acr-rad} = 10^{-6} M_\odot\ yr^{-1}$), and we do not consider it as a reasonable estimate for the disk evolutionary period we are interested in. Moreover, such high accretion rate would be in contradiction with the assumption of no influence of the embedding environment onto disk itself. Nevertheless, the accretion (at high accretion rates) could supply a non-negligible amount of small grains, particularly, where the intrinsic ones have already disappeared. This leads to a slight enhancement of the opacity and gives rise to forming of different populations of the coagulated grains (Mizuno 1989). However, on the timescales we considered and with adopted accretion rates, the effects of the accretion are rather minor.

References

Baines, M.J., Williams, I.P., Asebiomo, A.S., 1965, MNRAS, 130, 63
Balbus, S.A., Hawley, J.F., 1991, ApJ, 376, 214
Bath, G.T., Pringle, J.E., 1981, MNRAS, 194, 967
Bell, K.R., Lin, D.N.C., 1994, ApJ, 427, 987
Blum, J., Münch, M., 1993, Icarus, 106, 151
Blum, J., Wurm, G., Kempf, S., Henning, Th., 1996, submitted to Icarus
Cabot, W., Canuto, V.M., Hubickyj, O., Pollack, J.B., 1987a, Icarus, 69, 387
Cabot, W., Canuto, V.M., Hubickyj, O., Pollack, J.B., 1987b, Icarus, 69, 423
Cassen, P., Moosman, A., 1981, Icarus, 48, 353
Cassen, P., Pettibone, D., 1976, ApJ, 208, 500
Chandrasekhar, S., 1961, Hydrodynamic and Hydromagnetic Stability, Clarendon Press, Oxford
Chokshi, A., Tielens, A.G.G., Hollenbach, D., 1993, ApJ, 407, 806
Cuzzi, J.N., Dobrovolskis, A.R., Champney, J.M., 1993, Icarus, 106, 102
Deulfhard, P., 1985, SIAM Rev., 27, 505
Deulfhard, P., Wulkow, M., 1989, IMPACT Comput. Sci. Eng., 1, 269
Dubrulle, B., Morfill, G.E., Sterzik, M., 1995, Icarus, 114, 237
Duschl, W.J., Gail, H.P., Tscharnuter, W.M., 1995, submitted to A&A
Epstein, P.S., 1923, Phys. Rev., 22, 710
Frank, J., King, A.R., Raine, D.J., 1992, Accretion Power in Astrophysics, Cambridge University Press, Cambridge
Gail, H.P., Sedlmayr, E., 1988, A&A, 206, 153
Gardiner, C.W., 1990, Handbook of Stochastic Methods, Springer-Verlag, Berlin, Heidelberg, New York
Goldreich, P., Ward, W.R., 1973, ApJ, 183, 1051
Henning, Th., Stognienko, R., 1996, A&A, 311, 291
Krause, F., Rädler, K.-H., 1980, Mean-Field Magnetohydrodynamics and Dynamo Theory, Akademie-Verlag, Berlin
Krause, F., Rüdiger, G., 1974, Astron. Nachr., 295, 93
Landau, L.D., Lifschitz, E.M., 1988, Hydrodynamics, Nauka, Moscow (in Russian)
Landau, L.D., Lifschitz, E.M., Pitajevski, L.P., 1988, Physical Kinetics, Nauka, Moscow (in Russian)
Larson, R.B., 1984, MNRAS, 206, 197
Lenzuni, P., Gail, H.P., Henning, T., 1995, ApJ, 447, 848
Lin, C.C., 1961, Statistical Theories of Turbulence, Princeton University Press, Princeton.
Lin, D.N.C., Papaloizou, J., 1980, MNRAS, 191, 37
Lin, D.N.C., Papaloizou, J., 1985, On the Dynamical Origin of the Solar System. In: Black D.C., Matthews M.S. (eds.) Protostars and Planets II, Univ. of Arizona Press, Tucson, 981
Lin, D.N.C., Pringle, J.E., 1987, MNRAS, 225, 607
Lüst, R., 1952, Z. Naturforschung, 7a, 87
Lynden-Bell, D., Pringle, J.E., 1974, MNRAS, 186, 799
Markiewicz, W.J., Mizuno, H., Völk, H.J., 1991, A&A, 242, 286
Mathis, J.S., Rumpl, W., Nordsieck, K.H., 1977, ApJ, 217, 425
Mizuno, H., 1989, Icarus, 80, 189
Mizuno, H., Markiewicz, W.J., Völk, H.J., 1988, A&A, 195, 183
Morfill, G.E., 1985, Physics and Chemistry in the Primitive Solar Nebula. In: Lucas, R., Omont, A. (eds.) Birth and Infancy of Stars, North-Holland, Amsterdam, 693
Ohtsuki, K., Shigeru, I., 1990, Icarus, 85, 499
Ossenkopf, V., 1991, A&A, 251, 210
Ossenkopf, V., 1993, A&A, 280, 617
Ossenkopf, V., Henning, T., 1994, A&A, 291, 943
Preibisch, T., Ossenkopf, V., Yorke, H.W., Henning, T., 1993, A&A, 279, 577
Pollack, J.B., McKay, C.P., Christofferson, B.M., 1985, Icarus, 64, 471
Rossi, S.C.F., Benevides-Soares, P., Barbuy B., 1991, A&A, 251, 587
Ruden, S.P., Lin, D.N.C., 1986, ApJ, 308, 883
Ruden, S.P., Pollack, J.B., 1991, ApJ, 375, 740
Safronov, V.S., 1969, Evolution of the Protoplanetary Cloud and Formation of the Earth and the Planets, Nauka, Moscow (in Russian)
Shakura, N.I., Sunyaev, R.A., 1973, A&A, 24, 337
Shu, F.H., Adams, F.C., Lizano, S., 1987, ARA&A, 25, 23
Stone, J.M., Hawley, J.F., Gammie, C.F., Balbus, S.A., 1996, ApJ, 463, 656
Tanaka, H., Nakazawa, K., 1994, Icarus, 107, 404
Völk, H.J., Jones, F.C., Morfill, G.E., Röser, S., 1980, ApJ, 85, 316
von Weizsäcker, C.F., 1944, Z. Astrophysik, 22, 319
von Weizsäcker, C.F., 1947, Z. Astrophysik, 24, 181
von Weizsäcker, C.F., 1948, Z. Naturforschung, 3a, 524
Weidenschilling, S.J., 1977, MNRAS, 180, 57
Weidenschilling, S.J., 1980, Icarus, 44, 172
Weidenschilling, S.J., 1984, Icarus, 60, 553
Weidenschilling, S.J., 1988, Formation Processes and Time Scales for Meteorite Parent Bodies. In: Kerridge, J.F., Matthews, M.S. (eds.) Meteorites and the Early Solar System, Univ. Arizona Press, Tucson, 348
Weidenschilling, S.J., 1997, submitted to Icarus
Weidenschilling, S.J., Ruzmaikina, T.V., 1994, ApJ, 430, 713
Wetherill, G.W., 1990, Icarus, 88, 330

This article was processed by the author using Springer-Verlag LaTeX A&A style file *L-AA* version 3.